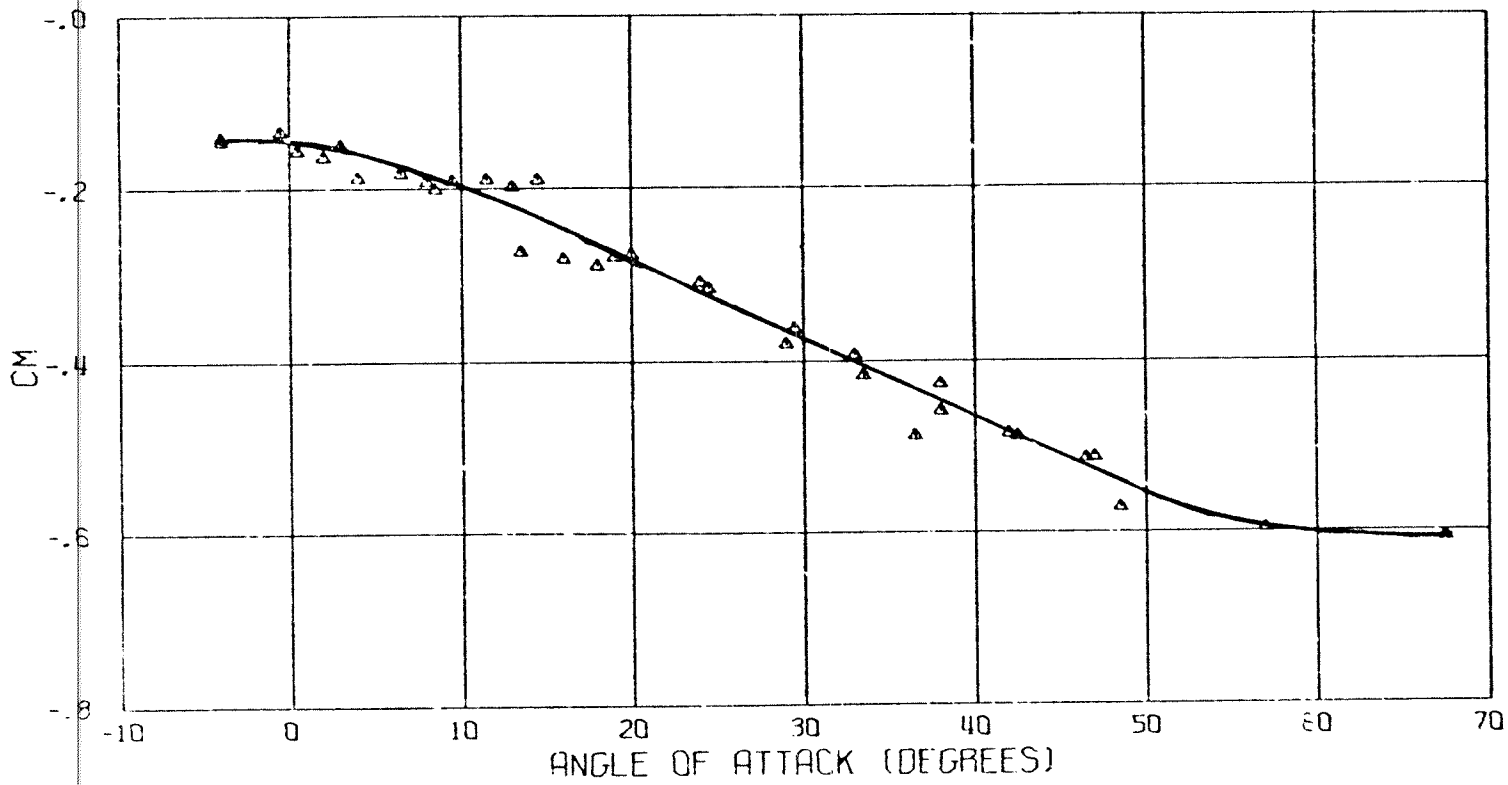

Figure 114. AR 3.0 C_m vs α

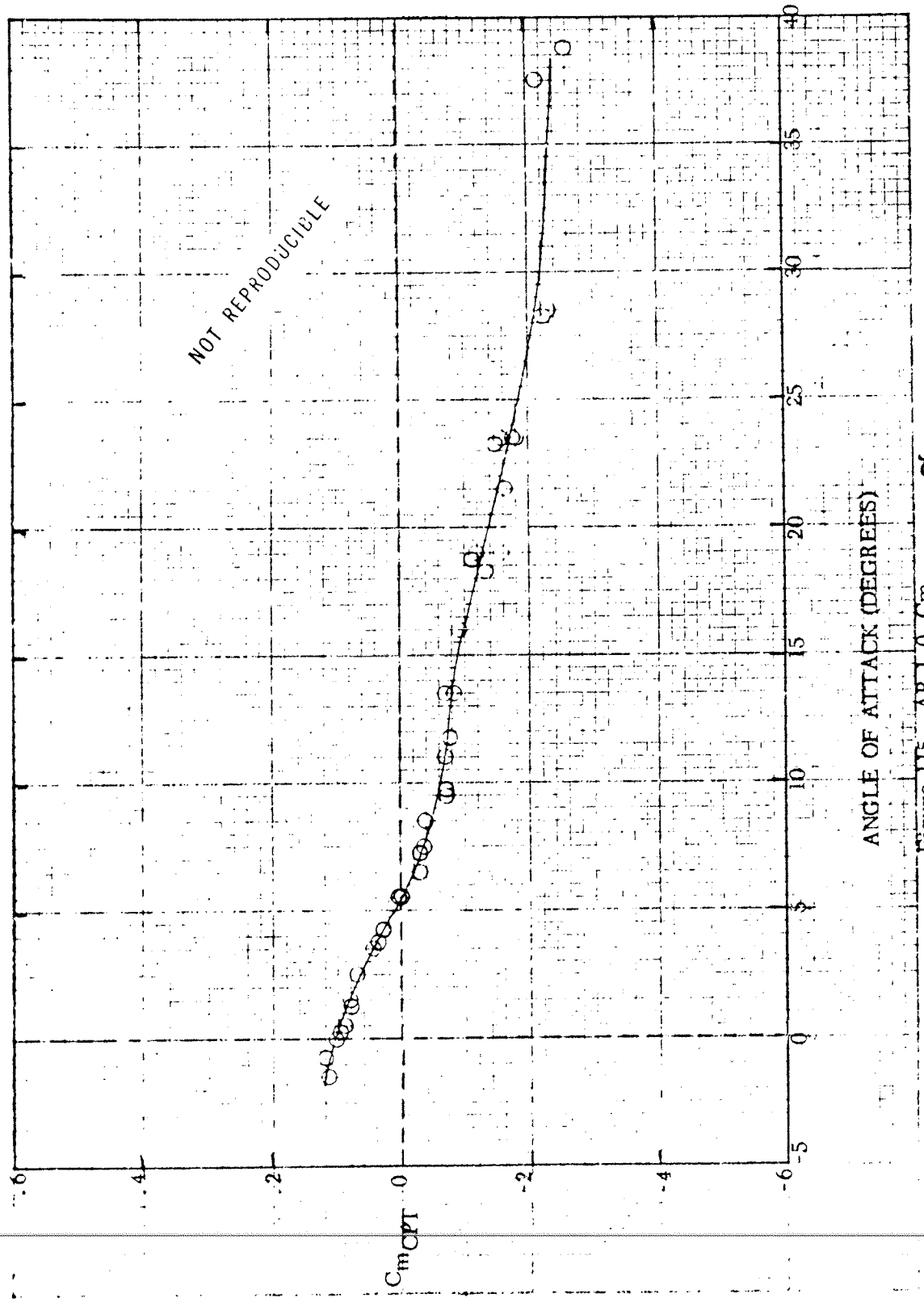

Figure 115. AR 1.0 $C_{m_{CPT}}$ vs. α

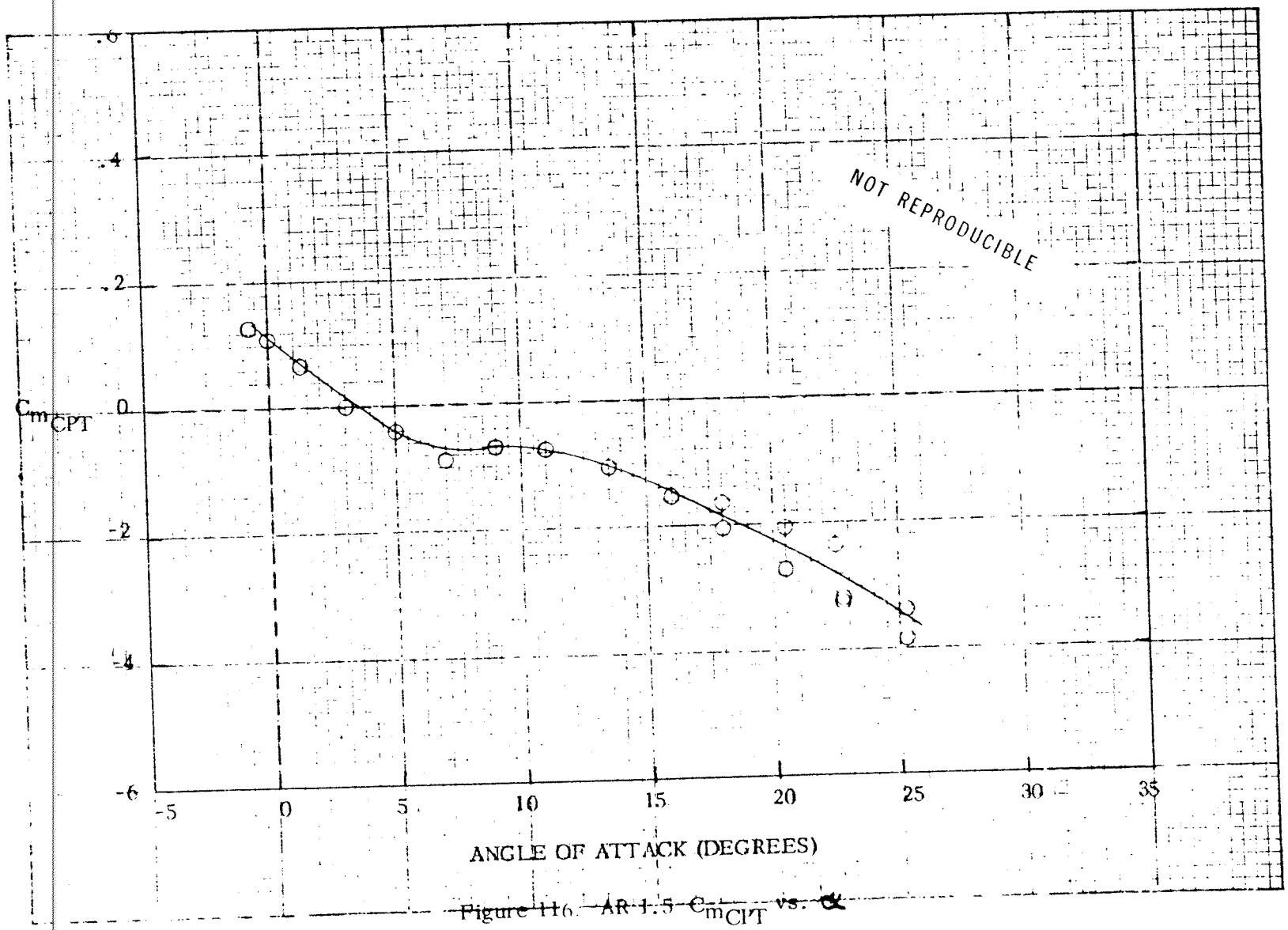

Figure 116 AR 1.5 $C_{m_{CPT}}$ vs. α

151

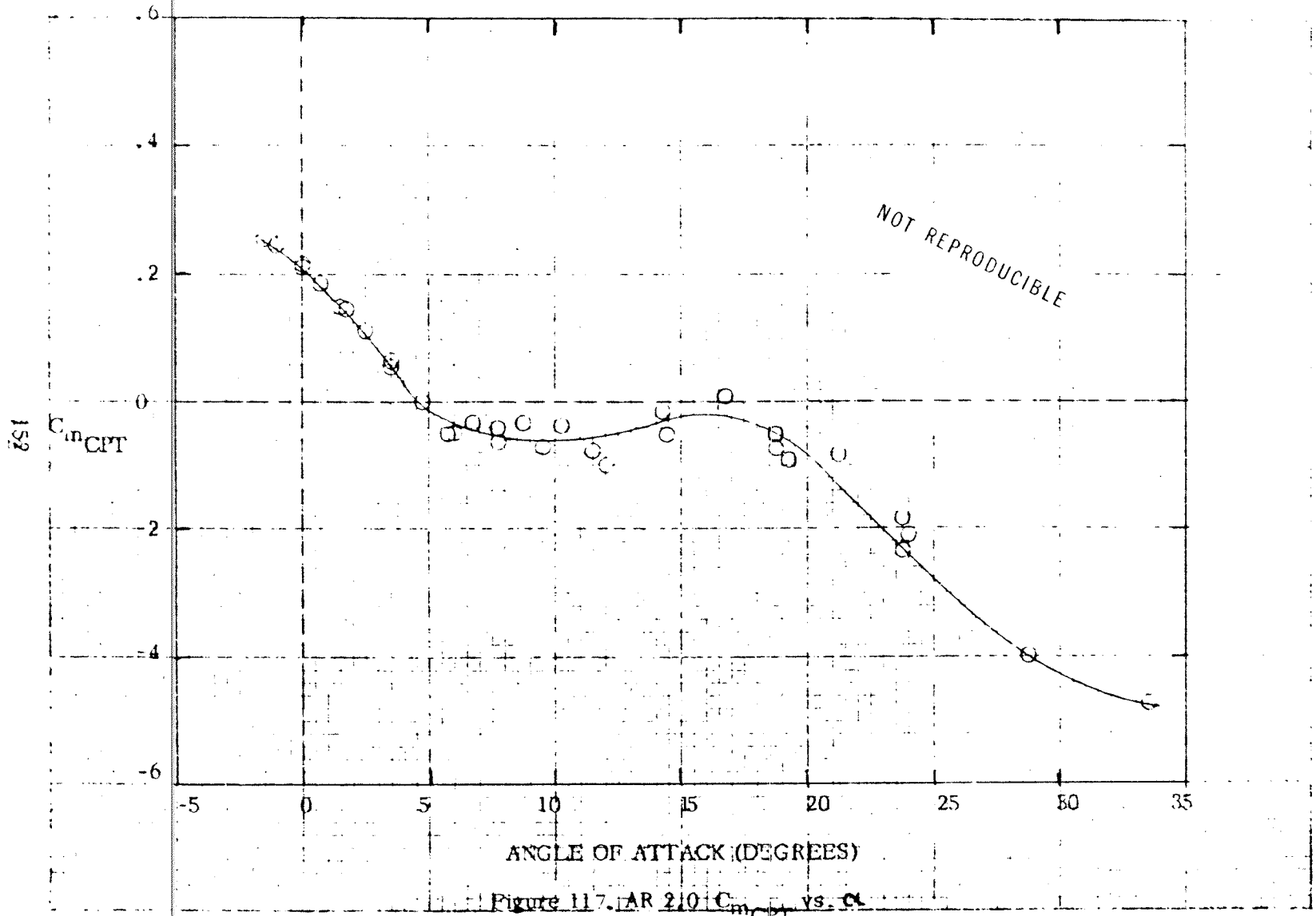

Figure 117. AR 2.0 $C_{m_{CPT}}$ vs. α

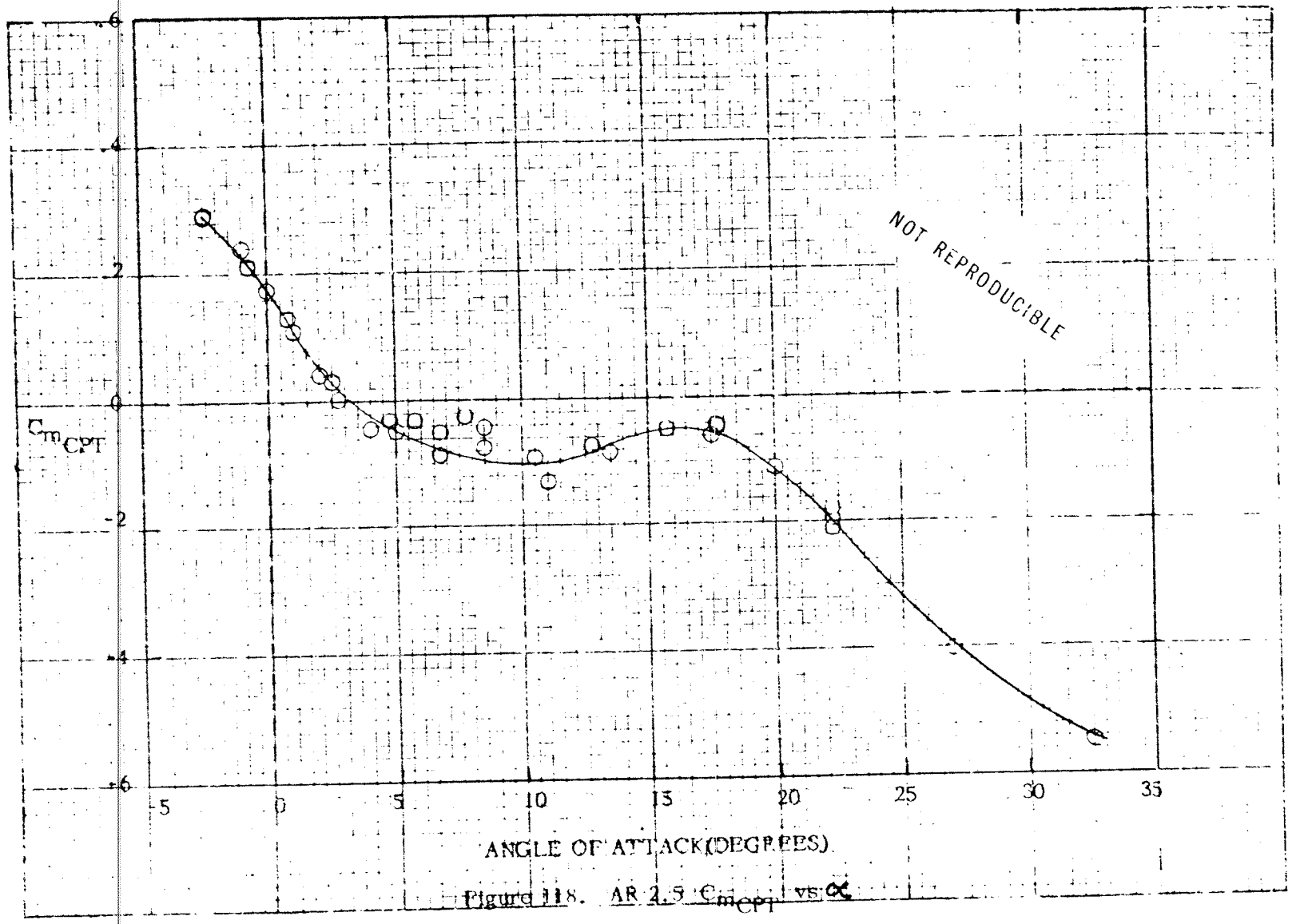

Figure 118. AR 2.5 $C_{m_{CPT}}$ vs α

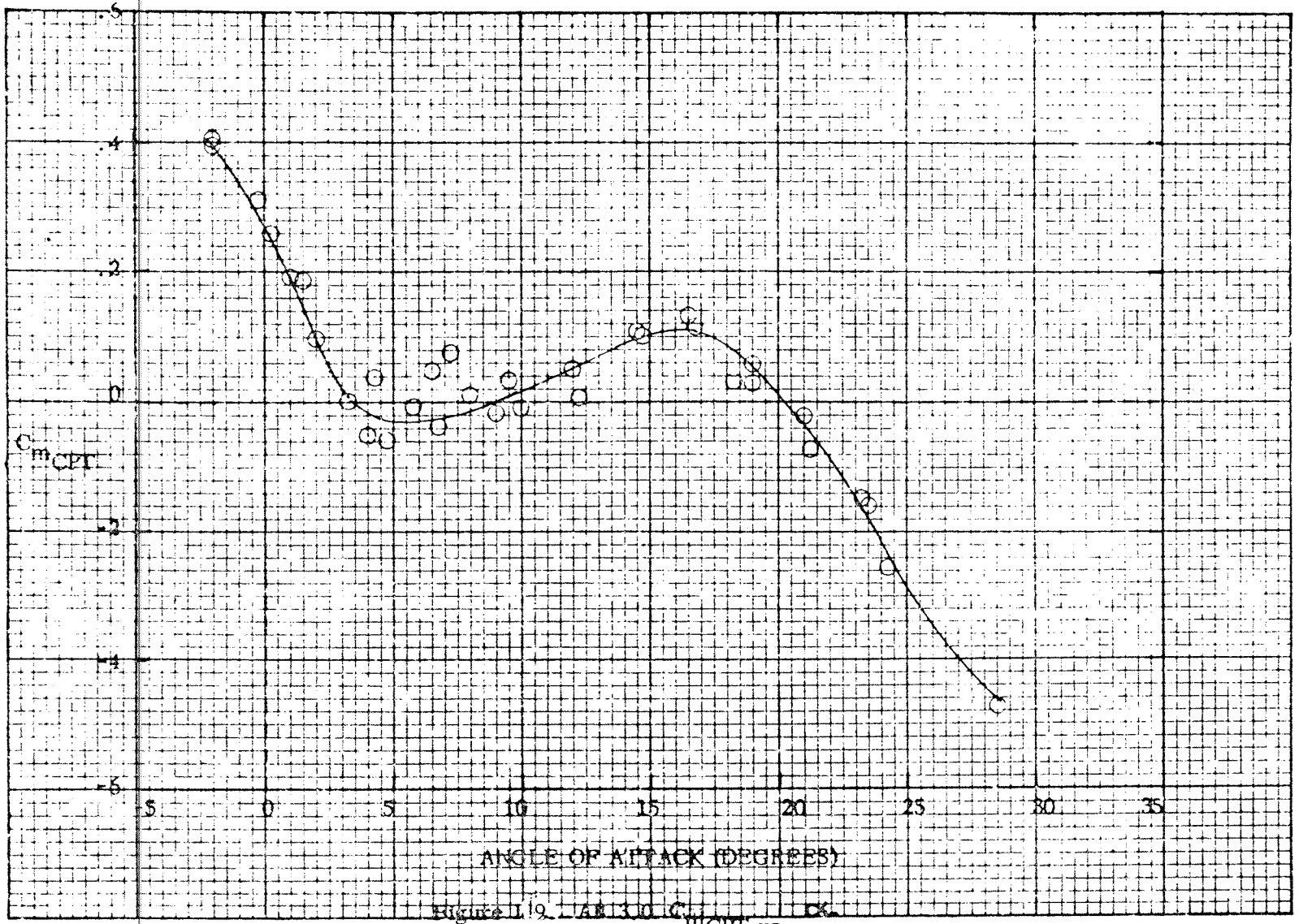

Figure I.9. AR 3.0 $C_{m_{CPT}}$ vs.

APPENDICES

APPENDICES

APPENDIX I

Transformation of Moment Coefficients About Confluence Point

The stability axes systems used in the development and presentation of the NASA Langley data and the positive direction of forces, moments, and angles are given in Figures I-1 and I-2.

As the Para-Foil moves through an air mass, forces are generated due to the dynamic reaction on the air similar to the forces associated with the wings of an airplane. These generated aerodynamic forces are known as the lift and drag forces of general airfoil theory.[12] When considered as a resultant force acting at the center of pressure varying with attitude, a moment about the lateral axis is introduced (Figure I-1). This moment is known as the pitching moment and affects the longitudinal stability of the Para-Foil.[13,14,15]

If the Para-Foil is flying directly aligned with the wind, the lift and drag are the only fluid forces generated. However, if this is not the case, additional forces are generated which act perpendicular to the lift and drag. This occurs when the relative wind is making some angle to the Para-Foil centerline (angle of sideslip, β). The resultant of these forces acting in the lateral plane is the side force, and depending upon its position and orientation with respect to the center of mass, additional moments are created. The moment tending to rotate the Para-Foil about its longitudinal axis is known as the rolling moment; about the vertical axis is known as the yawing moment (Figure I-1).[13,14,15]

The various moment coefficients are usually obtained experimentally in wind tunnel testing techniques about an arbitrary chosen reference point. Sometimes, as in the case of the Parafoil, it becomes advantageous to transfer the moment information to another point in the system (when a stability analysis of the total system is desired). For the Parafoil this point is the confluence point (CPT), that is, the point where all suspension lines are joined together and the payload is located Figure I-3.

Longitudinal Stability

The primary factor relating to longitudinal stability is the pitching moment, hence the following development outlines the derivation of the pitching moment about the CPT. To determine the pitching moment about the CPT consult Figure I-3. Summing moments about the CPT yields:

$$M_{CPT} = qSC_A \bar{z} - qSC_N x \tag{1}$$

in coefficient form:

$$cC_{M_{CPT}} = \bar{z} C_A - xC_N$$

$$= \bar{z} C_A - (\bar{x} + x_{CP}) C_N \tag{2}$$

$$= \bar{z} C_A - \bar{x} C_N - x_{CP} C_N \tag{3}$$

From Figure I-3 the following geometric relationship can be determined:

$$C_N = C_R \cos (\gamma_1 - \alpha) \tag{4}$$

with

$$cC_{m_{ref}} = - aC_R$$

$$C_R = - (\frac{c}{a}) C_{m_{ref}} \tag{5}$$

hence

$$C_N = -\left(\frac{c}{a}\right) C_{m_{ref}} \cos\left(\gamma_1 - \alpha\right) \tag{6}$$

Now

$$x_{CP} = \frac{a}{\cos\left(\gamma_1 - \alpha\right)} \tag{7}$$

Therefore from equations (6) and (7)

$$x_{CP} C_N = -cC_{m_{ref}} \tag{8}$$

and upon substitution of (8) into (3), results

$$cC_{m_{CPT}} = \bar{z}C_A - \bar{x}C_N + cC_{m_{ref}} \tag{9}$$

and upon division of the chord length, c, becomes

$$C_{m_{CPT}} = \frac{\bar{z}}{c} C_A - \frac{\bar{x}}{c} C_N + C_{m_{ref}} \tag{10}$$

where the independent variable is the angle of attack, α . For a given α , the coefficients C_L, C_D, and $C_{m_{ref}}$, are measured. Knowing these values, the axial force coefficient, C_A, and the normal force coefficient, C_N, are determined from the geometry of figure I-3.

$$C_A = C_R \sin\left(\gamma_1 - \alpha\right) \tag{11a}$$

$$C_N = C_R \cos\left(\gamma_1 - \alpha\right) \tag{11b}$$

where

$$C_R = \sqrt{C_L^2 + C_D^2} \tag{12}$$

$$\gamma_1 = \arctan\left(C_D/C_L\right) \tag{13}$$

Hence, returning to equation (10) $\bar{x}$ and $\bar{z}$, the horizontal and vertical distances to the CPT from the reference point respectively, are the only remaining unknown parameters of the right hand side.

For the scope of this analysis, all tests were conducted with $\bar{z} = 1.5b$. Corresponding to this vertical distance there is only one value of $\bar{x}$ associated with a condition of longitudinal balance. This condition of longitudinal balance occurs when $C_{m_{CPT}} = 0$.[14] Imposing this condition on equation (10) and solving for $\bar{x}$ yields,

$$\bar{x} = \frac{cC_{m_{ref}} + \bar{z} \; C_A}{C_N} \tag{14}$$

where the coefficients $C_{m_{ref}}$, C_N, and C_A are the values corresponding to the angle of attack at which C_L/C_D is a maximum. The Para-Foil is then rigged to fly at this trim angle-of-attack, which yields its best performance.

The behavior of the pitching moment about the CPT versus α will then determine the static longitudinal stability of the Para-Foil. Mathematically this corresponds to the sign and magnitude of the slope C_{m_α}, where a negative slope implies static longitudinal stability.[14]

Directional Stability

When the Para-Foil is at an angle of sideslip, β, relative to its flight path, the yawing moment produced must be such as to restore it to symmetric flight. If the yawing moment coefficient is as shown in figure I-2 the requirement for static directional stability is that the slope C_{n_β} be positive.[14] Hence to determine the yawing moment about the CPT, see figure I-4.The side force coefficient and yawing moment coefficient are measured about the reference point to be respectively, C_y and C_n. The side force coefficient acts perpendicular to the longitudinal plane which gives rise

to the yawing moment coefficient which acts in the lateral plane. Therefore, summing moments (coefficient form) about the CPT yields:

$$C_{n_{CPT}} = C_{n_{ref}} - \frac{x'}{b} C_y \quad (15)$$

where the geometry gives

$$x' = r \sin (\alpha + \epsilon) \quad (16)$$

$$r = \sqrt{\bar{x}^2 + \bar{z}^2} \quad (17)$$

$$\epsilon = \arctan (\bar{x}/\bar{z}) \quad (18)$$

Lateral Stability

When rolling oscillations occur the problem is one involving the lateral stability of the Para-Foil. If the rolling moment coefficient is as shown in figure F-2 the requirement for lateral stability is that the slope (Cl_{ϕ}) be negative.[14] To determine the rolling moment about the CPT reference Figure F-4 The rolling moment coefficient is measured about the CPT to be $C_{\ell_{ref}}$ and acts in the vertical plane. Hence, summing moments (coefficient form) about the CPT results in:

$$C_{\ell_{CPT}} = C_{\ell_{ref}} + \frac{z'}{b} C_y \quad (19)$$

$$z' = r \cos (\alpha + \epsilon) \quad (20)$$

For a vehicle as the Para-Foil, the stability derivatives involving rolling moment and yawing moment will reflect the influence of the wing side force and sideslip characteristics to a considerable extent, whereas the pitching stability derivative depends upon the lift and drag forces. In transferring this moment information about the confluence point, the effect of the suspension lines is included. Whether or not the additional drag due to the lines produce a stabilizing or destabilizing response is still open to analysis and testing.

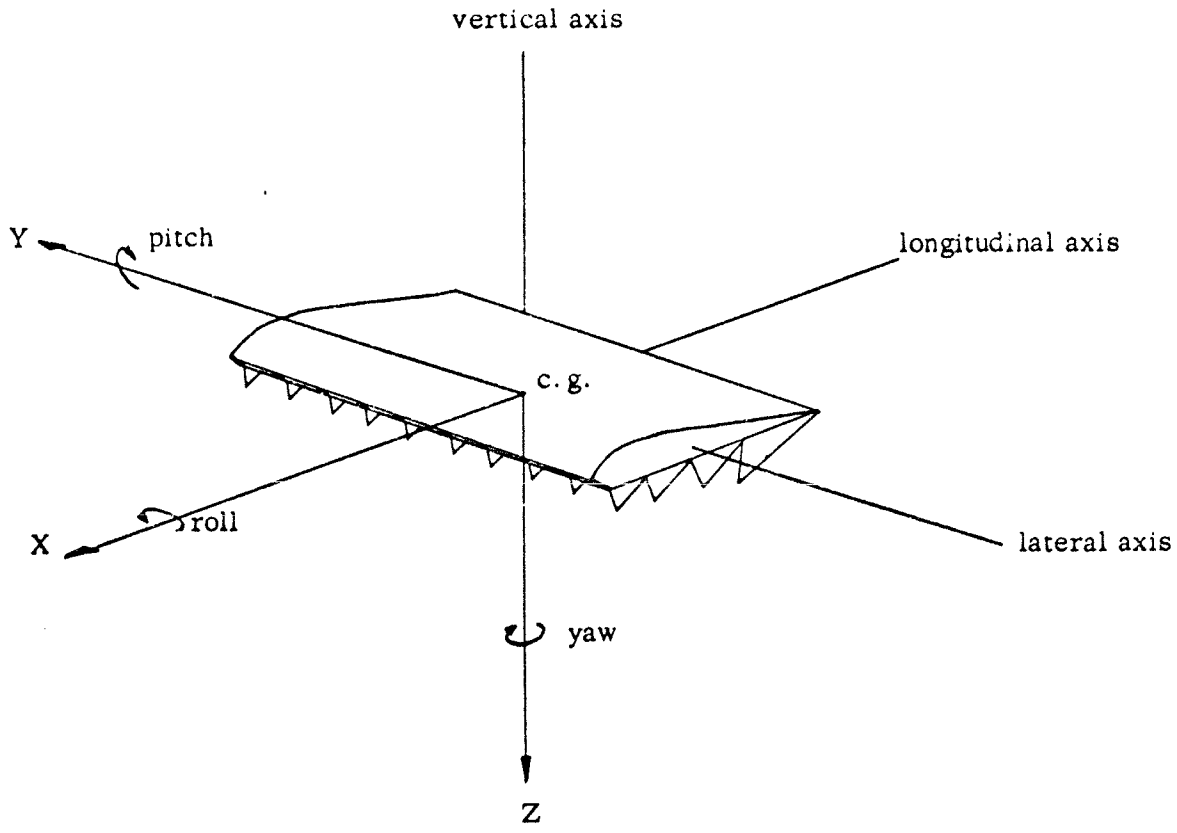

Figure I-1 Para-Foil Axis System (Body Axes)

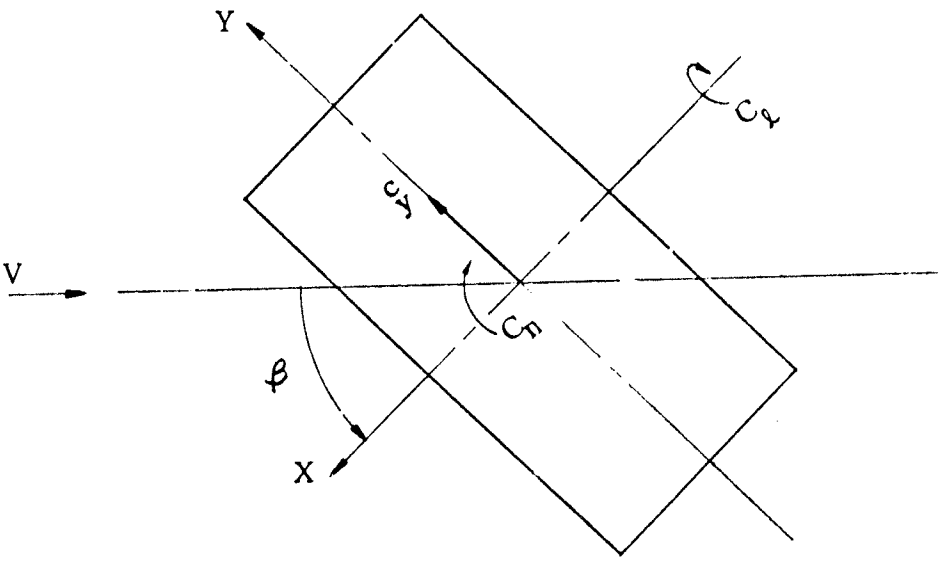

a) Directional and Lateral Forces and Moments (Pure Yaw)

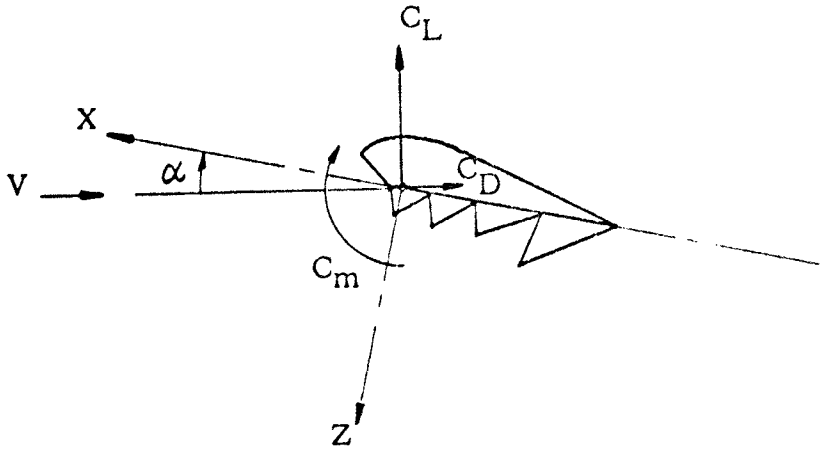

b) Longitudinal forces and moments (Pure Pitch)

Figure I-2. Axes Systems and Convention used to define positive sense of forces, moments, and angles. Longitudinal data are referred to wind axes and lateral data are referred to body axes.

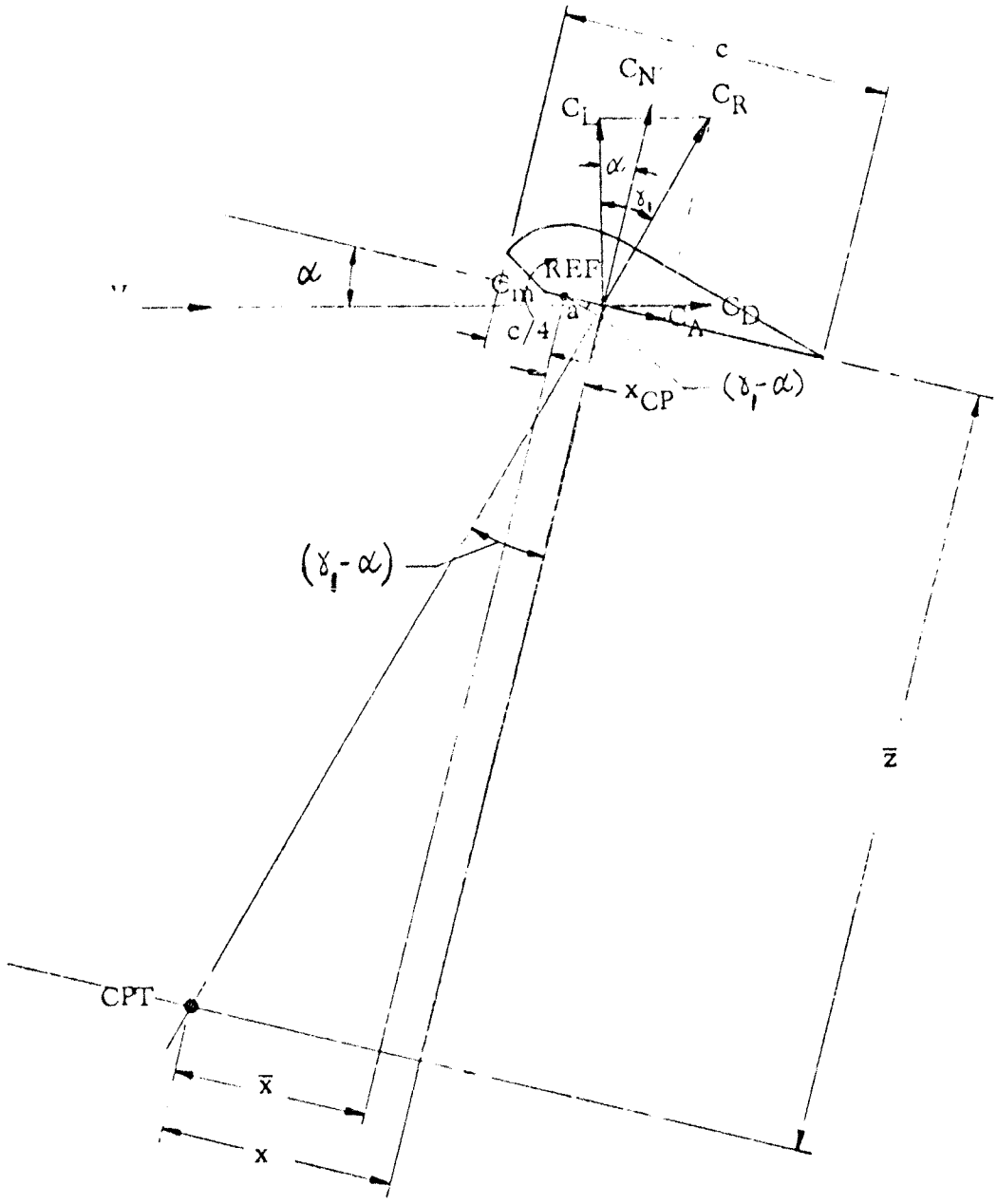

Figure 1-3Longitudinal stability analysis geometry.

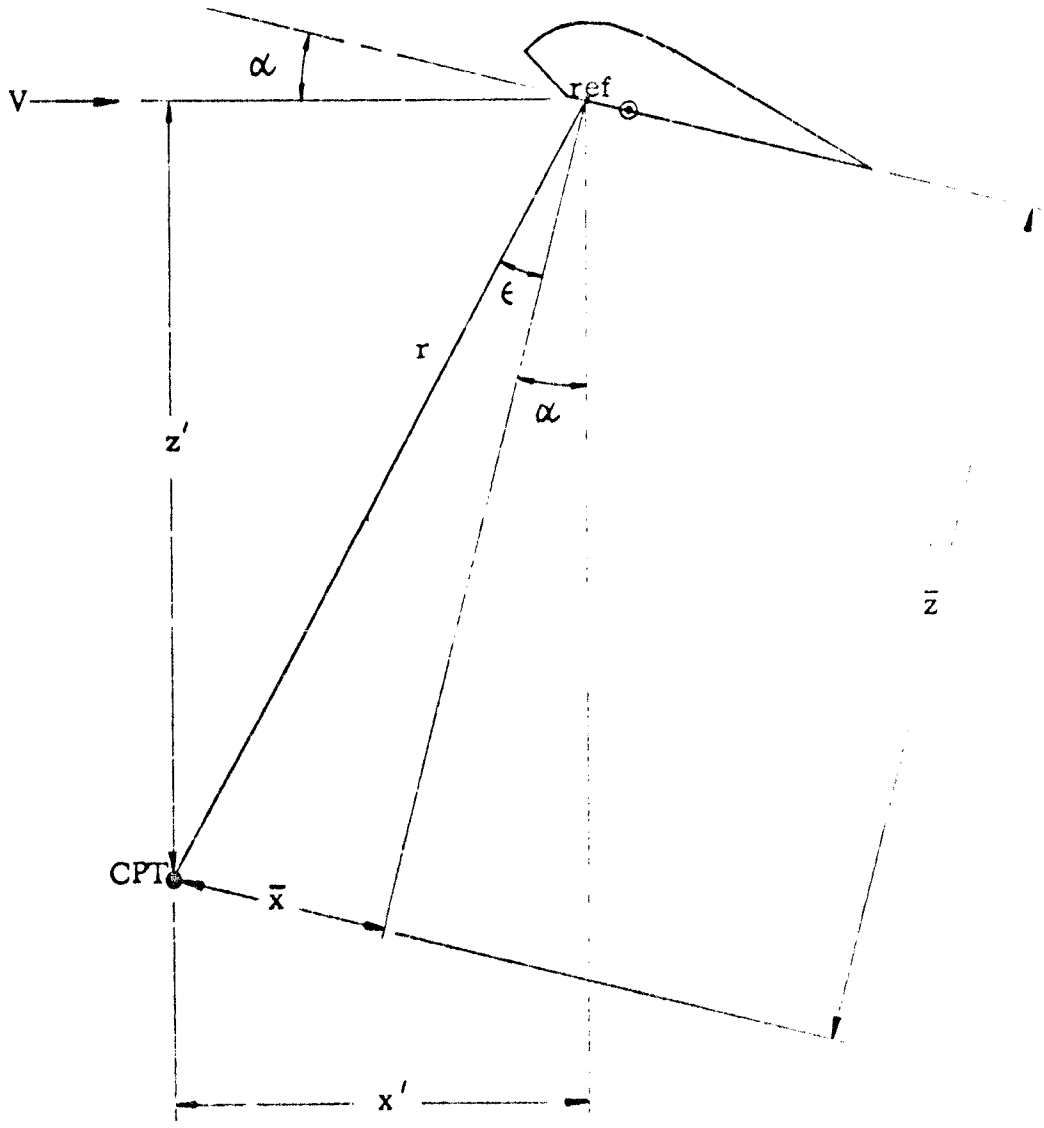

Figure I-4. Directional and Lateral Stability Analyses Geometry. Side force Acting downward at the reference.

APPENDIX II

LINE DRAG ANALYSIS - REMOVAL

NASA-Langley (Series Two): Tether Phase

The length of line exposed to the airflow was determined in the following manner. Reference Figure II-1 and Table II-1. Given the geometry in Figure II-1, h is determined accordingly:

$$h = \underline{L} \cos (\alpha + \theta_R) - (21.3 - \mathcal{Y}) \tag{1}$$

Knowing h, ℓ can be determined, as follows:

$$\ell = \frac{\underline{L}\, h}{h + (21.3 - \mathcal{Y})} \tag{2}$$

Assuming the air flow turns an angle of 10° and also that the incremental length, $\Delta \ell$, is perpendicular to the j-streamline,

$$\Delta \ell = x \sin 10^{\circ} \tag{3}$$

$$\text{where} \quad x = (21.3 - \mathcal{Y}) \tan (\alpha + \theta_R) \tag{4}$$

Then $(\ell + \Delta \ell)$ is the length of one of the A-suspension lines exposed to the airstream. Consulting the rigging schematic (Figures 17-21, main report) the total frontal area of all the suspension lines exposed to the airstream is:

$$S_{sus} = (n\ 375)\ (\ell + \Delta \ell)\ (dia_{375}) + (n_{550})\ (\ell + \Delta \ell)\ (dia_{550}) \tag{5}$$

Note that all the suspension line lengths exposed are assumed to be of equal length and all are assumed to be fully exposed to the airstream. All lines were also assumed not to stretch.

The control lines of each unit are joined together at a wing on each side of the Parafoil a distance ξ below the trailing edge. From these rings two primary control lines run down to the controller. Hence the frontal area of exposed control line lengths is

$$S_{cont} = (n_{cont})\ (\xi)\ (dia_{375}) + 2\ (2\Delta\ell)\ (dia_{375}) \tag{6}$$

where the distance from the ring to the j-streamline is assumed to be $(2\Delta\ell)$.

For the two guide lines a length of 300 feet per guide line was assumed exposed to the airstream. Hence the frontal area is:

$$S_{guide} = 2\ (30)\ (dia_{375}) \tag{7}$$

The total frontal area of all lines exposed to the airflow is then:

$$S_{line} = S_{sus} + S_{cont} + S_{guide} \tag{8}$$

Assuming a drag coefficient of 1.0 (from Hoerner) for the line based on the line frontal area, the drag coefficient of the line drag based on wing planform area can be computed, as follows:

$$D = q\ S_{line}\ C_{D_\pi} \tag{9a}$$

$$D = q\ S_{wing}\ C_{D_S} \tag{9b}$$

$$S_{line}\ C_{D_\pi} = S_{wing}\ C_{D_S}$$

$$C_{D_S} = \frac{S_{line}}{S_{wing}}\ C_{D_\pi} \tag{10}$$

The component of this drag coefficient that contributes to the drag of the system is $(C_{D_S} \cos \alpha)$ and hence this drag component was subtracted from the given data drag coefficient to yield the drag coefficient of the Parafoil

alone.

Some tests of the variable aspect ratio unit were conducted with 100 pound test line. When these situations occurred the same procedure was followed in removing the line drag, noting the diameter of 100-line to be 0.040 inches.

All computations were programmed and run on the University of Notre Dame's Univac 1107 computer.

NASA Langley (Series Two): Strut Phase

The length of line exposed to the airflow is

$$\ell = 0.339L \tag{11}$$

where L is the length given in Table II-1 and mentioned in the Tether Testing Phase. (Figure II-2)

The resulting frontal area is determined as in the preceeding tether analysis, and hence the line drag coefficients based on wing planform area are found. All computations were performed on the Univac 1107 computer.

NASA-Langley (Series One)

The length of lines exposed to the airstream was determined from the geometry of the various test configurations.[3] All lines were assumed to be fully exposed to the airstream and not to stretch. Knowing the lengths and line diameters the total frontal area of the lines was determined. In a manner similar to that of the previous section the drag coefficient of the suspension lines based on wing planform area was computed and then subtracted from the total drag yielding the drag of the Para-Foil wing only.

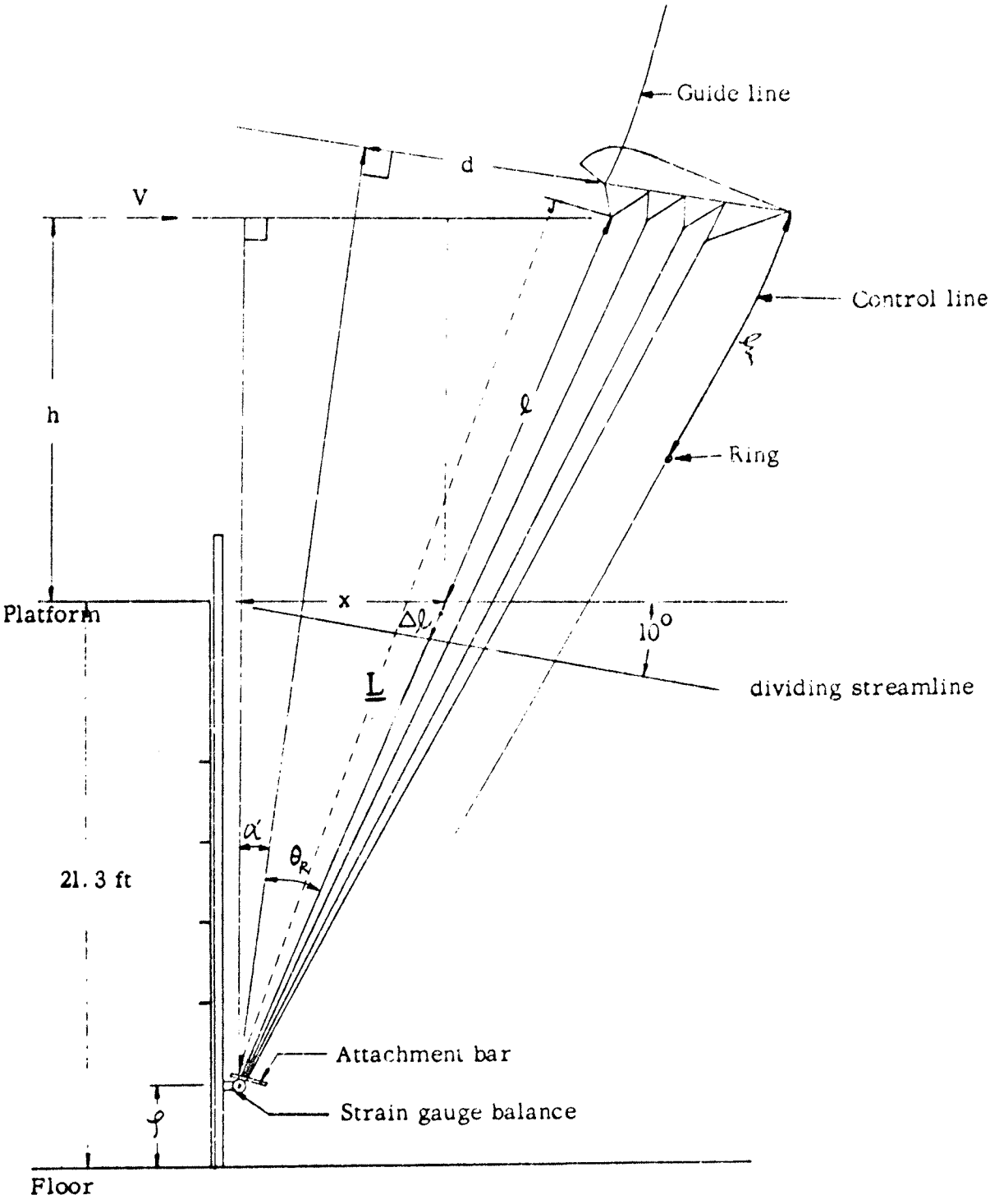

Figure II-1. Tether Testing Line Drag Determination.

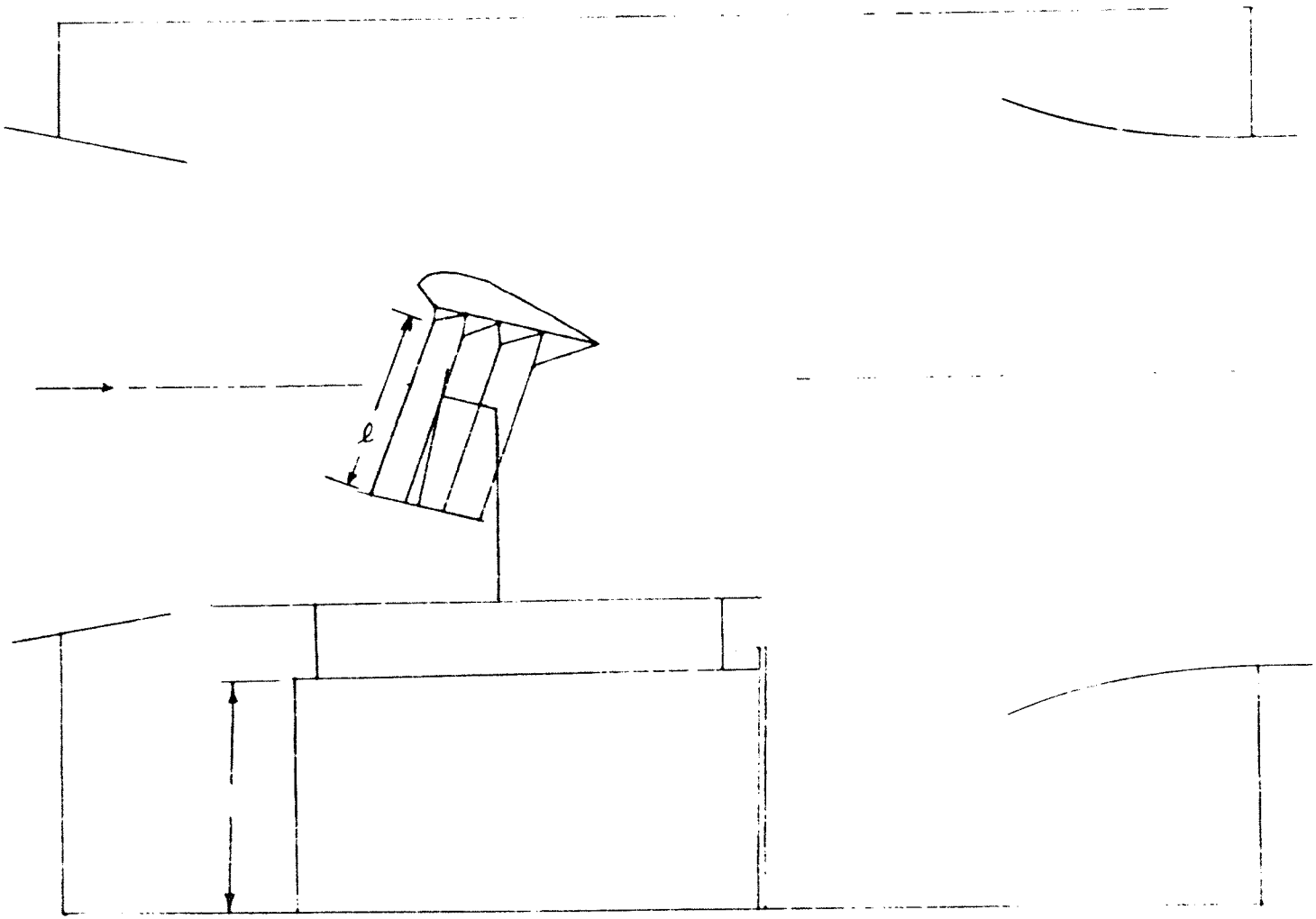

Figure II-2. Sketch of Strut Test Configuration in Langley Full Scale Tunnel

TABLE II-1

Model Description and Information

MODEL	f (in feet)	r_f (in feet)	θ_R (in degrees)	L (in feet)	DESCRIPTION
Basic AR 1.0	15	8	31	20.13	Orange w/green flares
Basic AR 1.5	12	9	26.6	23.95	White w/orange flares
Basic AR 2.0	9	10	21.8	26.84	Orange w/green flares
Basic AR 2.5	6	11	16.7	29.28	White w/orange flares
Basic AR 3.0	3	12	11.3	31.42	White w/center panel orange, alternating orange & white flares
Variable AR 3.0	3	12	11.3	31.42	green

VARIABLE	S (in feet)	# Flares	#550 lines	#375 lines	#100 lines
AR 3.0	147	13	9	4	39
AR 2.5	123	11	9	2	33
AR 2.0	87	9	9	0	27
AR 1.5	74	7	7	0	21
AR 1.0	49	5	5	0	15

APPENDIX III

LINE DRAG ANALYSIS - ADDITION

NASA - Langley (Series Two): Tether Phase

The length of line not exposed to the airstream was determined in the following manner. Reference Figure II-1 and Table II-1. Knowing the total length of the A-suspension lines ($\underline{L}$) and the length of line exposed to the airstream ($\ell + \Delta\ell$: from Appendix II), the difference yields the line not exposed to the airflow:

$$s = \underline{L} - (\ell + \Delta\ell)$$

where the same assumptions employed in Appendix II are incorporated. Hence, following the approach in Appendix II, the total frontal area of all suspension lines not exposed to the airflow is:

$$S_{\substack{\text{line} \\ \text{not} \\ \text{exposed}}} = S_{sus} + S_{cont} + S_{guide}$$

where

$$S_{sus} = S_{375} + S_{550}$$

$$= (n_{375})\,(s)\,(dia_{375}) + (n_{550})\,(s)\,(dia_{550})$$

$$S_{cont} = (2)\,(18)\,(dia_{375})$$

$$S_{guide} = 0$$

The remainder of the method is exactly similar to Appendix II but for the fact that the drag coefficient due to the unexposed lines is added to the given drag of the system.

NASA - Langley (Series Two): Strut Phase

The same procedure as Appendix II was followed except for:

$$\underline{L} - \ell = 0.661\ \underline{L}\ .$$

APPENDIX IV

NOTRE DAME MODEL

DRAG DATA CORRECTION

Upon completion of the analysis conducted in preparation for this report it was discovered that Parafoil models used in the tests conducted at Notre Dame included drag producing protuberences which were not taken into consideration in developing the drag or the lift-to-drag data. The purpose of this appendix is to present the effects of correcting the data to reflect removal of this additional drag.

Inspection of models 3 and 4 employed in the Notre Dame tests (see Table II and Figure 8) reveals that four nuts, two bolts, and aluminum flares of 24 ga. thickness were employed, the drag contributions of which were not previously taken into account. Accordingly, the incremental reduction in drag coefficient due to these proturbences is given in Figure IV-1. A new summary of the drag data for Parafoils of aspect ratios 1.0 - 3.0 is given in Figure IV-2 and a new summary for the lift to drag ratio is given in Figure IV-3.

AR	$\Sigma \Delta C_D$	ΔC_D Nuts (4)	ΔC_D Bolts (2)	ΔC_D Flares
1	.04036	.0266	.00834	.00542
1.5	.02806	.01773	.00557	.00476
2.0	.02253	.0133	.0042	.00503
2.5	.01856	.01053	.00340	.00463
3.0	.01639	.00887	.00273	.00474

NUT: C_D = .80* A = 0.283 in.^{2} (2 of this area)
A = 0.132 in.^{2} (2 of this area)

BOLT C_D = 0.80** A = .1303 in.^{2} (2 of this area)

FLARE: C_D = 0.48*** ΔA = .5250 in.^{2} (AR = 2.0)

*Fluid Dynamic Drag, Hoerner, p.5-8, Fig. 14a
**Ibid, p.5-8, Fig. 13e
***Ibid, p.5-8, Fig. 13c

Figure IV-1. Protuberance Drag.

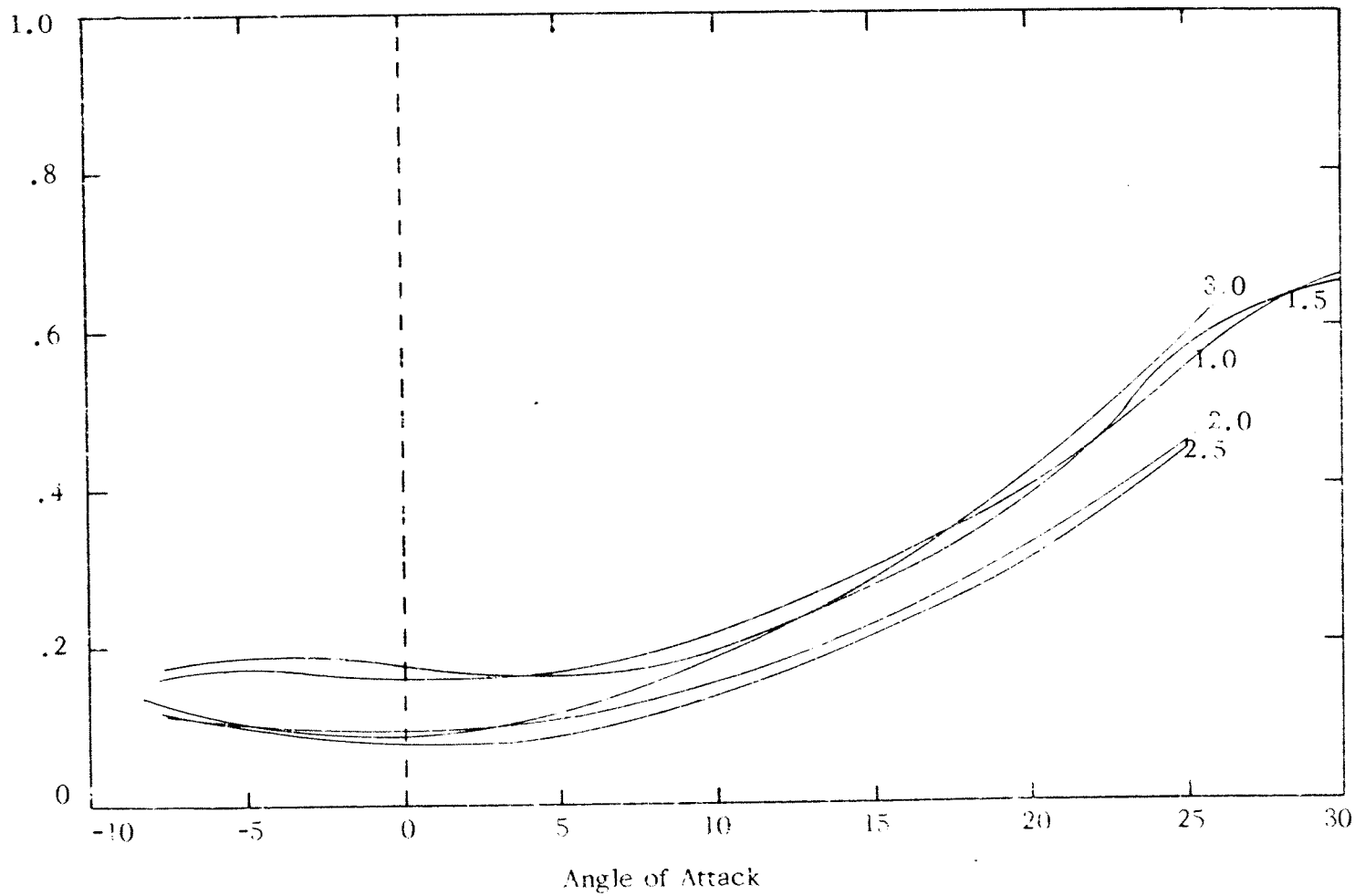

Figure IV-2. Summary of Coefficient of Drag (No Lines).

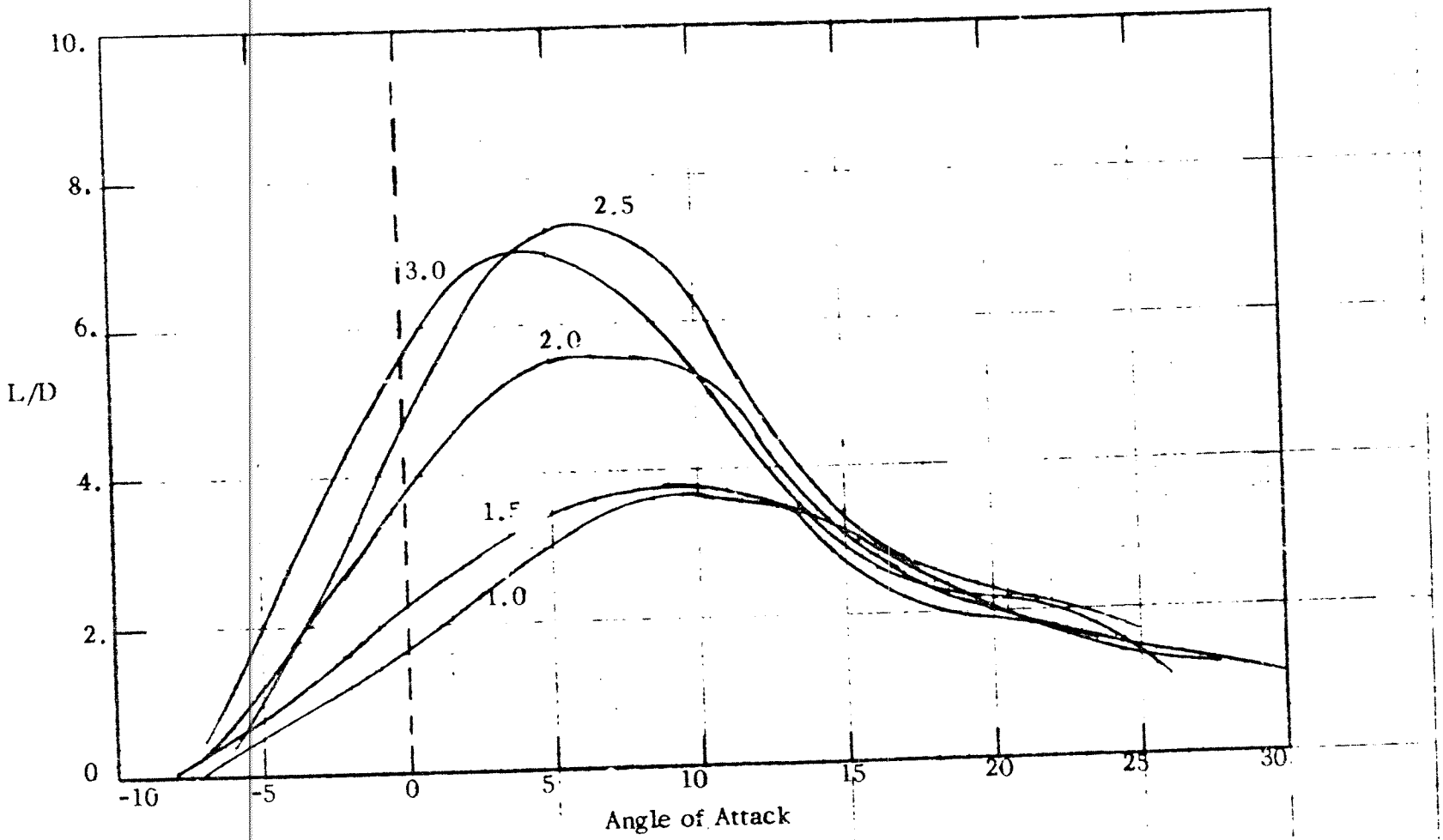

Figure IV-3. L/D Summary No Lines.

APPENDIX V

PARAFOIL FLIGHT PERFORMANCE

The aerodynamic data for the various Parafoil designs without line rag was given in the summary Figures 69, 70, 82 and 94. Correction of nese figures to reflect removal of drag due to model proturbences was resented in Appendix IV. In actual flight systems it is necessary to include rag created by lines and payload in predicting the overall system per- ormance. The purpose of this appendix is to illustrate incorporation of line rag for a personnel size Parafoil.

In considering the additional drag due to lines, a drag coefficient of one is used as was used in Appendices II and III. Although in actual practice, the drag coefficient is less than one due to the angle of the line to he flow field, line to line interference and improved separation points a drag coefficient of one was also used in these line drag calculations for consistency.

Figure V-1 illustrates the flight configuration of lines for the standard 200 sq.ft. jump Parafoil, ND 2.0 (200). It is noted that the line diameters are all .0125 ft., and that the total length of lines are reduced by cascading the rigging. The incremental drag coefficient due to incorporation of lines is .033. Based on the figures in Appendix IV and this line drag contribution, Figure V-2 illustrates the drag coefficient for the flight configuration together with the lift coefficient and the lift to drag ratio. Figures V-3 and V-4 provide similar aerodynamic data for the AR = 2.5 and AR = 3.0 Parafoils. A summary is provided in Figure V-5.

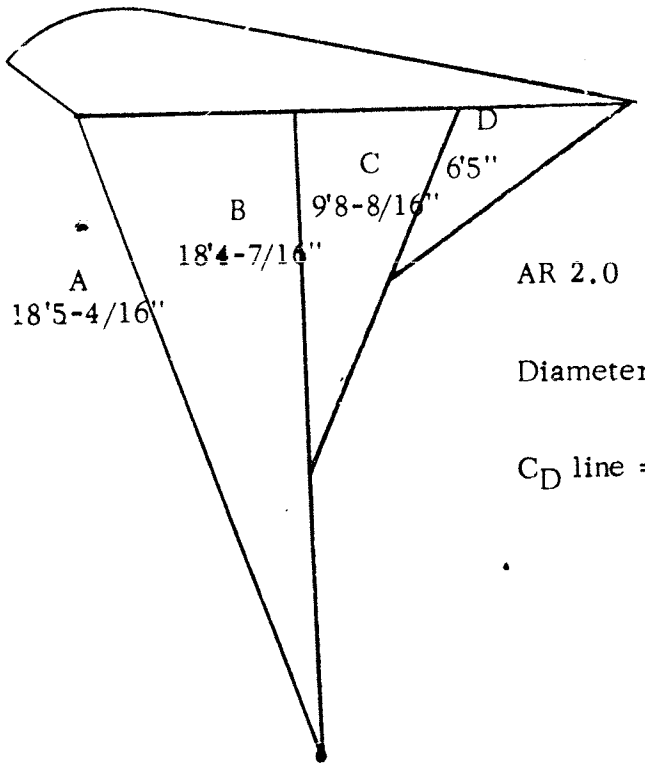

AR 2.0 (200 ft.^{2})

Diameter of line = .0125 ft.

C_D line = 1.0

Figure V-1. Line Drag Calculation AR 2.0.

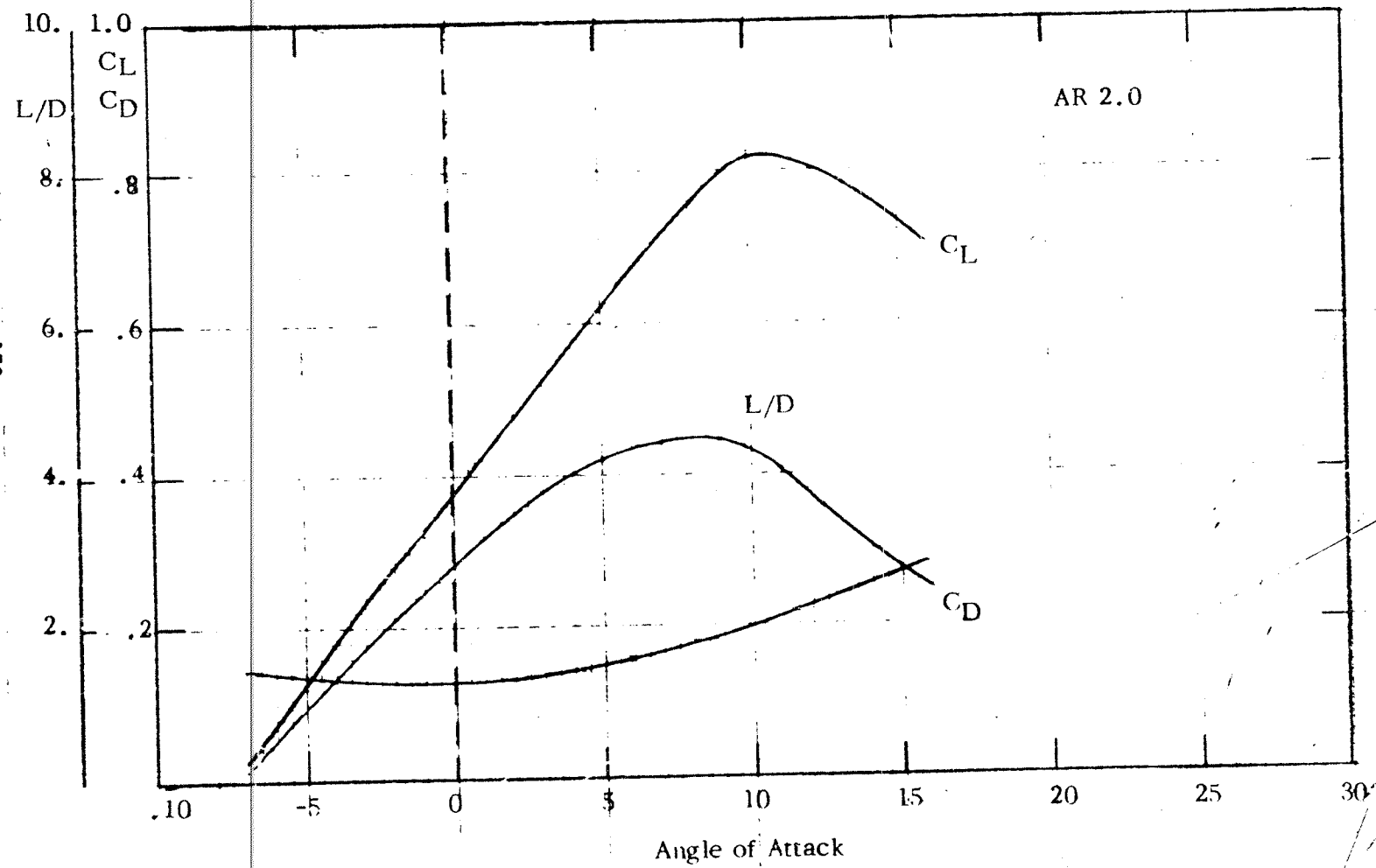

Figure V-2. — C_L, C_D and L/D for AR 2.0 With Lines.

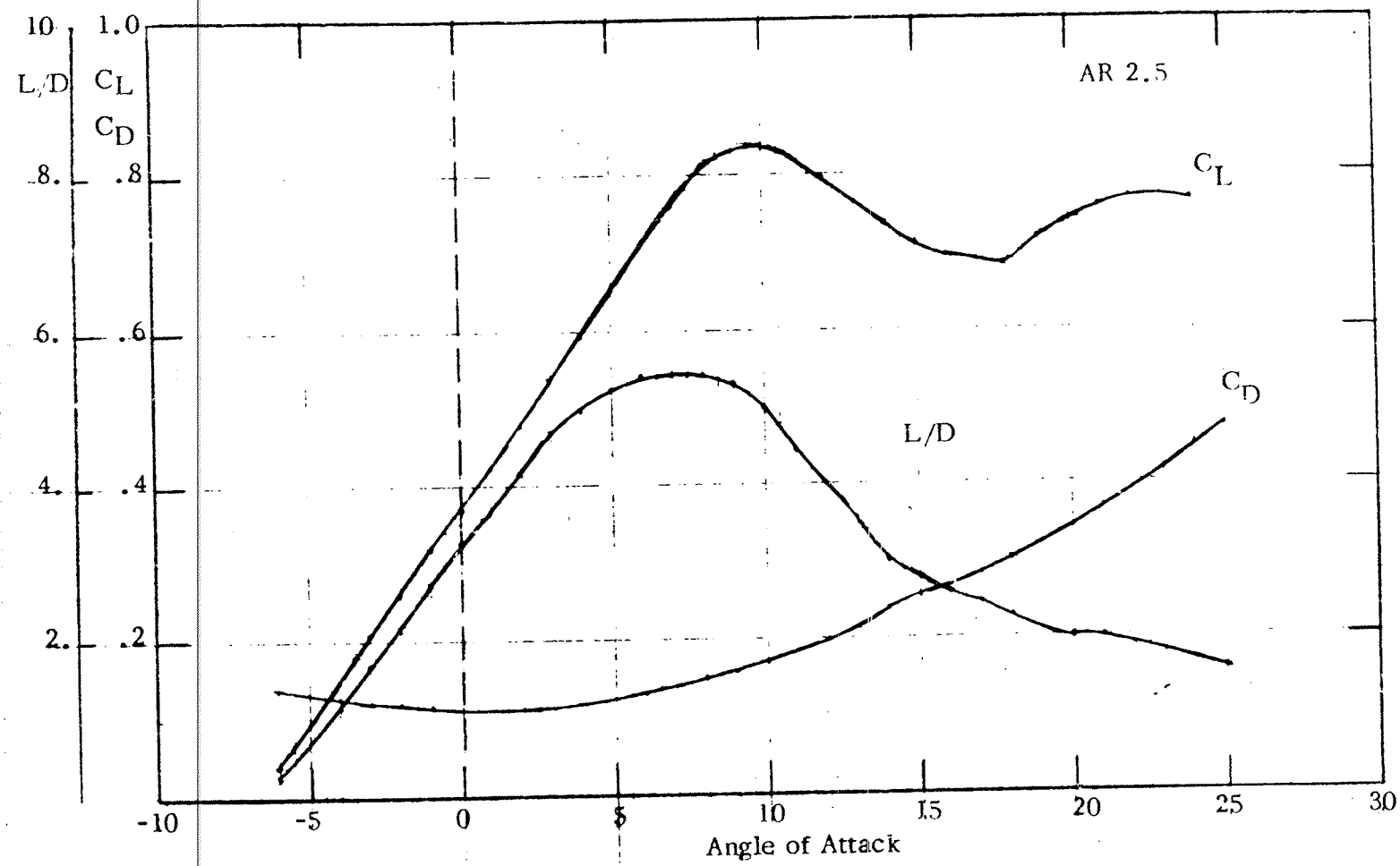

Figure V-3. C_L, C_D and L/D for AR 2.5 With Lines.

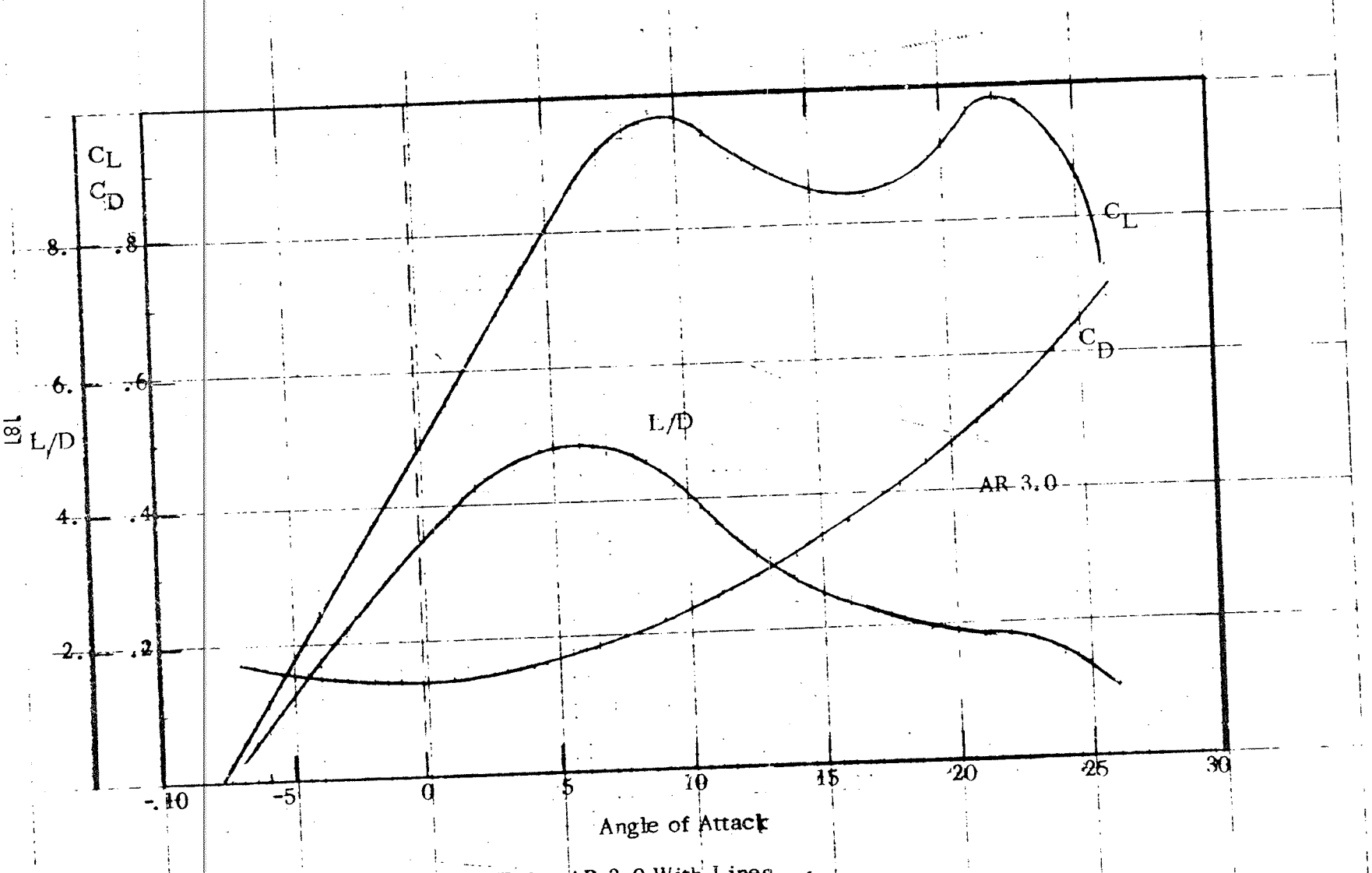

Figure V-4 . C_L , C_D and L/D for AR 3.0 With Lines

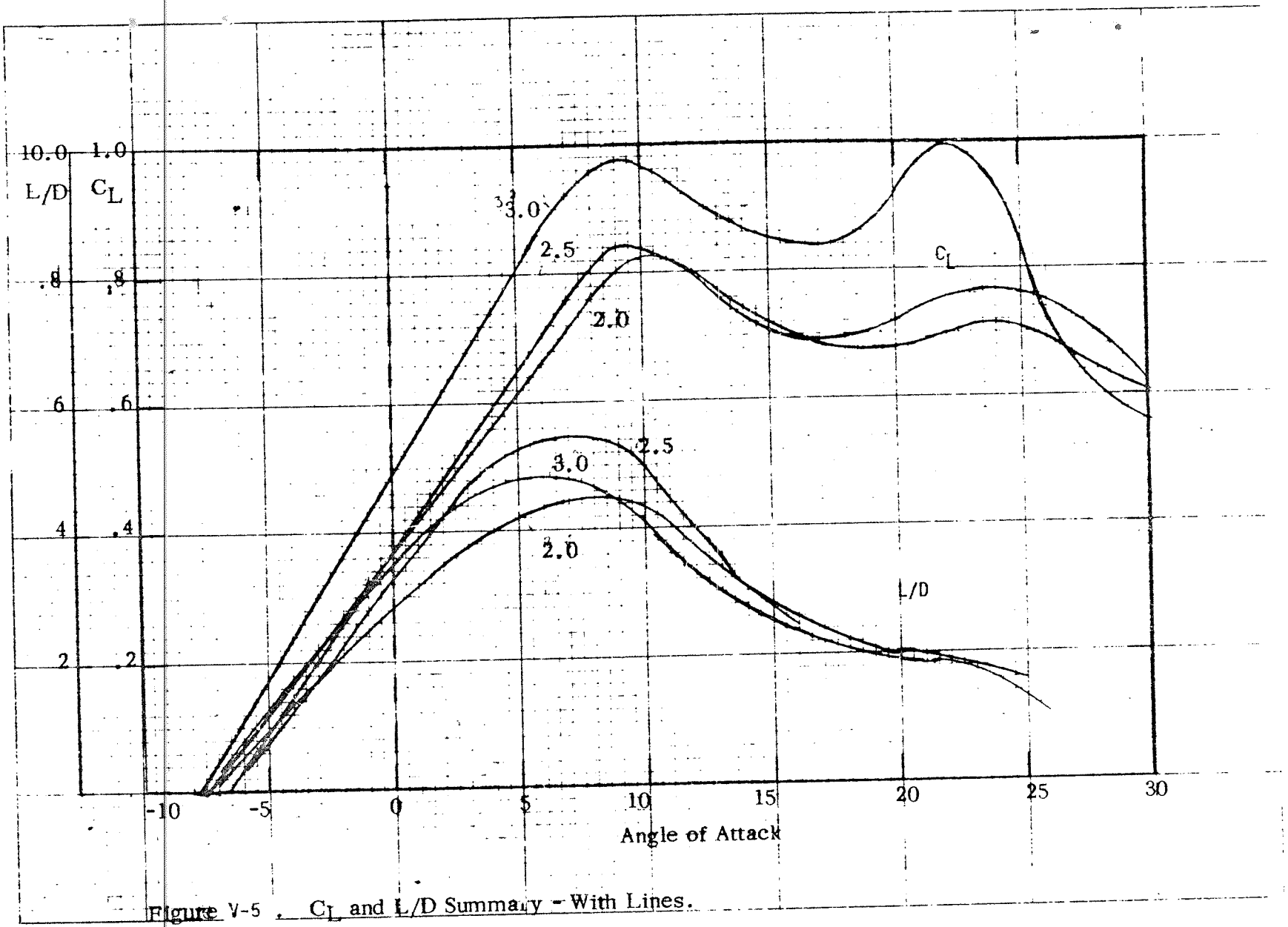

Figure V-5 . C_L and L/D Summary - With Lines.

REFERENCES

Nicolaides, John D., and Knapp, Charles F., A Preliminary Study of the Aerodynamic and Flight Performance of the Para-Foil, Conference on Aerodynamic Deceleration, University of Minnesota, July 8, 1965.

Nicolaides, John D., On the Discovery and Research of the Para-Foil, International Congress on Air Technology, Little Rock, Arkansas, November, 1965.

Burke, Sanger M., and Ware, George M., Static Aerodynamic Characteristics of Three Ram-Air Inflated Low Aspect Ratio Fabric Wings, Langley Research Center, Hampton, Virginia, NASA WP 264, July, 1966.

Pope, A., Wind Tunnel Testing, John Wiley and Sons, Inc., New York, April, 1964.

De France, Smith J., The NACA Full Scale Wind Tunnel, NACA Report 459, 1933.

Nathe, Gerald A., Knapp, Charles F., and Hall, Charles R., Wind Tunnel and Free Flight Testing of Para-Foil Model Number 125, Aero-Space Engineering Departmental Report, Notre Dame University, June, 1966.

Kang, W.H., On the Static Wind Tunnel Investigation of Small Para-Foil Models to Predict Flight Characteristics, Master's Thesis, Aero-Space Engineering Department, University of Notre Dame, Notre Dame, Indiana, May, 1968.

Walker, R.H., Static and Dynamic Characteristics of the Para-Foil as Determined from Pure Pitching Motion, Master's Thesis, Aero-Space Engineering Department, University of Notre Dame, Notre Dame, Indiana, July 1968.

Eikenberry, R.S., Analysis of Missile Dynamics Data, Part 1: Angular Motions, Sandia Laboratory Contractor Report, June, 1969.

Hoerner, S.F., Fluid Dynamic Drag, Published by author, 1965.

Sabersky, R.H. and Acosta, A.J., Fluid Flow, The Macmillan Co., New York, 1964, p.167.